INTERNATIONAL ATOMIC ENERGY AGENCY
UNITED NATIONS EDUCATIONAL, SCIENTIFIC AND CULTURAL ORGANIZATION

INTERNATIONAL CENTRE FOR THEORETICAL PHYSICS
34100 TRIESTE (ITALY) - P.O.B. 586 - MIRAMARE - STRADA COSTIERA 11 - TELEPHONE: 2240-1
CABLE: CENTRATOM - TELEX 460392 - I

SMR/302-23

COLLEGE ON NEUROPHYSICS:
"DEVELOPMENT AND ORGANIZATION OF THE BRAIN"
7 November - 2 December 1988

"An Analysis of a Silicon Model of Early Visual Processing"

John G. TAYLOR
University of Mathematics
King's College
London, UK

An Analysis of a Silicon Model of Early Visual Processing

J.G. Taylor

Depart. of Mathematics, King's College, London.

Requests for reprints should be sent to J.G. Taylor, Dept. of Mathematics, King's College, Strand, London WC2R 2LS, U.K.

An Analysis of a Silicon Model of Early Visual Processing

Abstract

A mathematical analysis is given of an analog model of retinal processing constructed recently in terms of a resistive lattice network by Mead and Mahowald. The basic equations are written down for a general lattice, and their continuum limit described. For linear resistors the general solution is given in terms of an arbitrary varying illumination input; special cases are discussed in detail.

Keywords: Retina, Machine Vision, Spatial Filter, Neural Model, Linear Network.

Introduction

Neuronal activity has usually been modelled in terms of the all-or-none response of a cell to incoming stimuli; the resulting firing patterns in networks of such cells arise from highly non-linear processes. However certain important aspects of visual processing, which occur at the retinal level, appear to be reasonably well described by a linear system. These aspects include the development of Mach bands (spatial enhancement of stimuli) and of transient peaks or troughs in response to the sudden increase or decrease of illumination respectively (temporal enhancement of stimuli). Such spatio-temporal enhancements of stimuli have been shown to arise from inhibitory connections in the retina both between neighbouring cells, and via feedback loops to the neuron under consideration ('self-inhibition'). The role of inhibitory interactions has been particularly well-studied in the case of the lateral eye of the horse-shoe crab (limulus polyphemus) (for a review see Hartline and Ratliff (1972)), but lateral inhibition also seems to occur in other invertebrate compound eyes, as well as in vertebrates (Dowling 1987); see also Ratliff (1965).

Lateral inhibition in the vertebrate retina is thought to arise from lateral connections in the initial stages of visual processing, by means of the horizontal cells. These latter form a dense arrangement of cells, called the outer plexiform layer, where incoming information is represented by analog signals. In the invertebrate retina the lateral and self-feedback connections form a dense layer of tissue called the lateral plexus. This is thought to contain collaterals from the axons of the eccentric

in the vertebrate retina

cells, which appear to play the role of the ganglion cells. The two types of retina are shown schematically in figs.1 and 2.

A very interesting hardware implementation of retinal inhibitory behaviour has recently been presented (Mead and Mahowald 1988), using a resistive network which connects the inputs from a set of photoreceptors, these latter responding logarithmically to the incident illumination. The resulting voltage is fed across a resistor and capacitance into a typical node of a hexagonal lattice. Each edge of the lattice is composed of a resistor; the general circuit is shown in Fig.3. The output consists of the amplified difference between the photoreceptor potential and that at the node. The results of Mead and Mahowald were obtained by using a silicon chip implementation of fig.3 with an experimental 48x48 pixel array. In order to understand this system better a mathematical analysis of the network is presented in this paper. It allows an extension of the results to a general class of lattices with inhibitory feedback, and so gives a way of finding the response for a whole range of such lattices without detailed hardware implementation.

THE BASIC EQUATIONS

The photoreceptor associated with the node P of the lattice is assumed to produce a potential $V_1(P,t)$. The resulting potential at P, $V_2(P,t)$, is obtained from the circuit of fig.4(a) in terms of the current flows I_1, I_2, I_3, where I_2 is the current in the capacitor C, and I_3 that entering the lattice at P. Let $I = f(V)$ be the resistor current for a potential V across its terminals. Initially f will be taken as described by a general S-shaped curve, but will be assumed linear in due course for detailed calculations. The current and potential differences between two points A, B in the lattice will be denoted respectively as I_{AB} (the current from A to B) and $V_{AB} = V_A - V_B$. Then from fig.4(a)

$$I_1 = f(V_{12})$$

$$I_2 = C\dot{V}_2$$

so that

$$I_3 = I_1 - I_2 = f(V_{12}) - C\dot{V}_2 \qquad (1)$$

From fig.4(b)

$$I_{PQ} = f(V_{PQ})$$

$$\sum_{<Q,P>} I_{PQ} = I_3(P) \qquad (3)$$

where the summation in (3) is over the six nearest neighbours in the hexagonal lattice of fig.3. Combining (1), (2) and (3), with $V_2(P) = V_P$, we obtain the basic equation

$$f(V_1(P) - V_P) - C\dot{V}_P = \sum_{<Q,P>} f(V_{PQ}) \qquad (4)$$

This is a system of first order linear differential equations for the set of functions $V_P = V(P,t)$, given the input potentials $V_1(P,t)$ for all P and t. As such they are expected to have

solutions in terms of the initial data $V_P(0)$ for a suitable class of smooth functions f.

It is to be noted that this model may be generalised to allow for more than nearest neighbour connections. For example in limulus (Hartline and Ratliff 1972) there is lateral inhibition from several neighbouring ommatidiae, with a Gaussian decrease in effect (see also Brodie, Knight and Ratliff, 1978a). A similar feature occurs in the vertebrate retina. Thus in general (4) may be extended to

$$f(V_1(P)-V_P)-C\dot{V}_P = \sum_Q f_{QP}(V_{PQ}) \qquad (5)$$

where f_{QP} depends essentially on the distance between Q and P, and the summation on the r.h.s. of (5) is no longer over nearest neighhbours only. A suitable choice for this weighting function, in the range where the resistor is linear, would be

$$f_{QP}(V) = G \exp[-d(Q,P)^2/a]V \qquad (6)$$

where G is a basic conductance constant and d(Q,P) is the distance between Q and P; a is the Gaussian spread of the lateral inhibition.

It is possible to linearise (4) in a range of values of the variables V_P sufficiently close to ongoing activity provided the input illumination $V_1(P)$ does not vary too rapidly. In the linear regime (4) becomes

$$G_1[V_1(P)-V_P]-C\dot{V}_P = G_2[NV_P - \sum_{<Q,P>} V_Q] \qquad (7)$$

In (5) the possibililty has been allowed of having different resistors in the lattice of fig.4(b) as compared to in the detector unit of fig.4(a); N is the number of neighbours to which each node is connected (6) in the case of Mead and Mahowald).

It is not clear whether the discrete lattice equations of (4) or (5) are an appropriate description of lateral inhibition. Be that as it may, it appears easier to handle the equations in a continuous version when working at the linearised level of (7). This requires re-expressing the r.h.s. of (7) in terms of spatial derivatives of V(P), now regarded as a differentiable function of the continuous real two-dimensional variable P. In the one-dimensional case,

$$2V_P - \sum_{<Q,P>} V_Q = -b^2V_P'' + O(b^4) \qquad (8)$$

where b is the distance between the nodes, in the limit as $b \to 0$. In the two-dimensional case

$$6V_P - \sum_{<Q,P>} V_Q = -\tfrac{3}{2}b^2\nabla^2V + O(b^4) \qquad (9)$$

where ∇^2 is the usual laplacian, $\nabla^2 = \partial^2/\partial x^2+\partial^2/\partial y^2$. Thus in the continuum limit, (7) becomes the system of second order linear partial differential equations

$$\dot{V} + (G_1/C)V - 3(G_2b^2/2C)\nabla^2V = (G_1/C)V_1 \qquad (10)$$

where terms $O(b^4)$ have been dropped from (10). The equations (10) will be analysed in the following section. The lattice will be taken to be infinite to avoid edge effects. ~~these also could be studied in either the discrete or continuous versions presented above.~~ The negative sign in front of the laplacian correctly indicates the presence of lateral inhibition, as will be seen.

t is possible to consider a continuous version of (6) or its
eneralisation to

$$\mathcal{S}_{P,P+\underline{r}}(V) = h(|\underline{r}|) \cdot V \qquad (10a)$$

here $\mathcal{S}_{P,P+\underline{r}}$ is now a density of contributions per unit rea. Then the coefficient of the laplacian on the r.h.s. of qp) is replaced by $\frac{1}{4}\int d^2\underline{r}.\underline{r}^2.h(|\underline{r}|)$, being a weighted sum $\frac{1}{4}\overline{r^2}$ of a quarter of the squared distances of nodes away from ach other. It is to be noted that in the hexagonal lattice case iscussed heretofore the weighted sum reduced to $\frac{3}{2}b^2$, as used n (9).

NETWORK RESPONSE

The most natural approach to the analysis of the system (10) is by means of Fourier transformation; this approach was basic in the analysis by Brodie et al of the limulus retina (Brodie,

Knight and Ratliff 1978b). If $\tilde{V}(\underline{k},w)$ is the Fourier transform of $V(\underline{r},t)$, where $\underline{r}$ denotes the two-dimensional position of the node,

$$\tilde{V}(\underline{k},w) = \int dt\, d^2r\, e^{-i(wt+\underline{k}.\underline{r})}V(\underline{r},t) \qquad (11)$$

then (10) becomes

$$[iw+(G_1/C) +3\underline{k}^2(G_2b^2/2C_1)]\tilde{V} = (G_1/C)\tilde{V}_1 \qquad (12)$$

with solution

$$\tilde{V} = [(iwC/G_1) + 1 +3\underline{k}^2(G_2b^2/2G_1)]^{-1}\tilde{V}_1 \qquad (13)$$

The transfer function

$$\mathcal{H}(\underline{k},w) = [(iwC/G_1) + 1 +3\underline{k}^2(G^2b^2/2G_1)]^{-1} \qquad (14)$$

may be compared to that of Brodie et al (1978b) (especially fig.4 of that reference) and with equation 10 of Brodie et al (1978a). $\mathcal{H}$ of equation (14) falls off more slowly for large w than does the corresponding function of Brodie et al (which behaves like $w^{-\theta}$); (14) also has a slower fall-off in $\underline{k}^2$, as $(\underline{k}^2)^{-1}$, compared to the Gaussian fall-off of Brodie et al (1978b).

By the Fourier inversion theorem and use of (13),

$$V(\underline{r},t) = (2\pi)^{-3}\int d^2k dw\left[1+iw\frac{C}{G_1}+3\underline{k}^2b^2\frac{C_1}{2G_2}\right]^{-1}\tilde{V}_1(\underline{k},w)e^{i(\underline{k}.\underline{r}+wt)} \qquad (15)$$

Thus V is known, at least formally, for any input V_1. Let us consider some special cases to compare with the results of Mead and Mahowald (1988) (who consider amplification of $V-V_1$):

(a) uniform illumination(step function in time)

In this case $\nabla^2V = 0$, and the solution is given as

$$V(P,t) = V(P,0)+(G_1/C)\int_0^t dt'V_1(P,t')\exp[-(G_1/C)(t-t')] \qquad (16)$$

For a temporal step function input

$$V_1(P,t) = a + f\theta(t) \qquad (17)$$

(where $\theta(t) = 0$ for $t < 0$, 1 for $t > 0$) (16) gives, with $V(P,0) = a$,

$$V_1(t) - V(t) = f \exp[-G_1 t/C]\,\theta(t) \qquad (18)$$

This response is shown in fig.5a, and may be compared with the response function of their figure 4(a) (large) of Mead and Mahowald (1988). The similarity is reasonable and is expected to be improved by the addition of non-linearity in the function $f()$ of eqn.(1) and on taking account of the actual shape of the illumination profile used by Mead and Mahowald (1988), where the θ-function in (17) is smoothed off. In particular this may lead to the rounding off of the initial sharp peak. It is to be added that in the case of uniform illumination all the nodes in the network change up together so the system has a single time constant, since there is no lateral current flow.

(b) general pixel illumination (step function in time)

One can show, with $\lambda^2 = 3b^2G_2/2G_1$ and $\rho(\underline{r})$ the spatial distribution of intensity of illumination, that

$$V_1(\underline{r},t) = \rho(\underline{r})[a + f\theta(t)] \qquad (19)$$

$$V(r,t) = aF_1(\underline{r}) + f\theta(t)F_2(\underline{r},t) \qquad (20)$$

$$F_1(\underline{r}) = (2\pi)^{-2}\int d^2\underline{k}\,\tilde{\rho}(\underline{k})[1+\underline{k}^2\lambda^2]^{-1}e^{i\underline{k}\cdot\underline{r}} \qquad (21a)$$

$$F_2(\underline{r},t) = (2\pi)^{-2}\int d^2\underline{k}\,\tilde{\rho}(\underline{k})[1+\underline{k}^2\lambda^2]^{-1}[1-\exp(-(1+k^2\lambda^2)tG_1/C)]e^{i\underline{k}\cdot\underline{r}} \qquad (21b)$$

In general these integrals cannot be evaluated, though one can see from (21) that

$$V_1(\underline{r},t) - V(\underline{r},t) = (2\pi)^{-2}\int d^2\underline{k}\,\tilde{\rho}(\underline{k})e^{i\cdot\underline{k}\cdot\underline{r}}\{[1-(1+k^2\lambda^2)^{-1}][a+b\theta(t)] + (1+k^2\lambda^2)^{-1}f\theta(t)e^{-(1+k^2\lambda^2)tG_1/C}\} \qquad (22)$$

The expression (22) will depend on the detailed form taken by $\rho(\underline{r})$, the input illumination distribution. ~~In general (22) will have a transient peak of height proportional to b, together with an asymptotic value proportional to (a+f). The fall-off from the transient peak will be expected to be steeper than in case (a).~~

The detailed form of (22) can be calculated if $\rho(\underline{r})$ is assumed to have a Gaussian distribution

$$\tilde{\rho}(\underline{k}) = e^{-k^2d^2} \qquad (23)$$

For $d \gg \lambda$ (when the width of the illuminated region is much larger than the space constant ~~effective lattice spacing~~) it is possible to evaluate (22) in powers of λ/d, with value

$$V_1(\underline{0},t) - V(\underline{0},t) = f\theta(t)e^{-tG_1/C} + V_1\frac{\lambda^2}{d^2} + O(\lambda^4/d^4) \qquad (24)$$

This has the behaviour shown in fig.5b. There is very close similarity to the results of Mead and Mahowald (1988) in that there is an initial peak whose height is independent of the size of the illuminated patch, and then an exponential decrease to a constant asymptotic value. It is to be noticed that this latter value decreases as the size of the patch increases, until in the limit as $d \to \infty$ (total illumination) case (a) is reached. Such behaviour is precisely that seen in Mead and Mahowald (1988), fig.4a. As in case (a) above the sharpness of the initial peak is expected to be removed by taking account of the detailed shape of the illumination increase and by non-linearity in f.

(c) Step function in space

The illumination is taken independent of time t but not of $\underline{r}$, so that (10) reduces to

$$V - 3(G_2b^2/2G_1)\nabla^2V = \rho(\underline{r}) \qquad (25)$$

In the one-dimensional case, with ρ a step function $\frac{\rho}{2}\theta(x-x_0)$, (25) has solution

$$V = \frac{\rho}{2} - \frac{1}{2}\rho e^{-x/\lambda} \qquad (x > 0) \qquad (26a)$$

$$= \frac{1}{2}\rho e^{+x/\lambda} \qquad (x < 0) \qquad (26b)$$

so that

$$V_1 - V = \frac{1}{2}\rho\left[e^{-x/\lambda}\theta(x) - e^{x/\lambda}\theta(-x)\right] \qquad (27)$$

This agrees closely with the corresponding fig.6 of Mead and Mahowald (1988) and the discussion associated with fig.7 of that reference.

The above discussion may be extended to the two dimensional case. For rotationally symmetric illumination it is possible to use cylindrical co-ordinates to solve (25), and instead of (27) obtain the solution (in distance units of λ)

$$V_1 - V = A I_0(r)\theta(r_0 - r) + B K_0(r)\theta(r - r_0) \qquad (28)$$

where I_0 and K_0 are the modified Bessel functions of the first and second kinds of order zero, and A B are constants given by

$$A = \rho K_0'(r_0)/J, \quad B = \rho I_0'(r_0)/J \qquad (28a)$$

with

$$J = I_0'(r_0) K_0(r_0) - I_0(r_0) K_0'(r_0) \qquad (28b)$$

The shape of (28) is similar to that of (27), with an extreme fall-off; near $r=r_0$ the behaviour shown for the extreme cases of $r_0 \sim 0$ and $r_0 \sim \infty$ in figure 6. It is to be noted that fig 6(b), for $r_0 >> 1$, corresponds indeed very closely to that

edge of the illuminated patch is going to infinity in this case. The other extreme, when has a different feature, in that the central value is close to twice that of the maximal interior value in case (b). This asymmetry between in and outside for case (a) is to be expected in that there is only a small central region from which to obtain external inhibition, whilst there is a very large external region to give central inhibition.

In particular it may be possible to obtain a value for $\langle \underline{r}^2 \rangle$, the mean squared effective connection distance between nodes, as described in the second and previous section, in particular associated with equation (34). This may be compared with the averaged observed distance between nearest neighbour horizontal cells to give a general measure of the overall range of connectivity between the horizontal cells.

(d) Moving edge

The response to a moving edge should show anticipatory effects

just before the on-transient, as noted by Brodie et al (1978a). Taking the edge moving along the x-axis with velocity v then

$$V_1(\underline{r},t) = a+f\theta(x-vt) \qquad (29a)$$

for which

$$\tilde{V}_1 = (2\pi)^3 a\delta^2(\underline{k})\delta(w) + f.(2\pi)^2.\delta(k_y)(-i/k_x).\delta(w+k_x v) \qquad (29b)$$

It is possible to compute from (29) and (15) that

$$V_1 - V = \frac{f}{\sqrt{4\lambda^2+\frac{v^2C^2}{G_1^2}}}\left[\left(\frac{1}{k_-}\right)e^{-k_-(x-vt)}\theta(x-vt) + \left(\frac{1}{k_+}\right)e^{-k_+(x-vt)}\theta(x-vt)\right] \qquad (30)$$

where

$$k_\pm = (1/2\lambda^2)\left[(vC/G_1) \pm [4\lambda^2+(v^2C^2/G_1^2)]^{\frac{1}{2}}\right]$$

Equation (30) reduces exactly to equation (27) when v = 0. The shape of the response (30) is similar to that of the second figure in fig.7 of Mead and Mahowald (1988) (though now with the transient moving with the edge at x = vt). It can also be compared with a very similar response to a stationary stimulus for an on-centre C-cell of a cat in fig.6(b) of that reference and with the in general more asymmetrical responses to moving stimuli for limulus in fig.15 of Brodie et al (1978a).

The actual shape of (30) may be obtained in the limits $v \sim 0$ or $v \sim \infty$, when

$$k_\pm \sim \frac{1}{\lambda}\left(\pm 1 + \frac{vC}{2G_1\lambda}\right) + O(v^2) \qquad (v \sim 0) \quad (31a)$$

$$k_\pm \sim \frac{vC}{G_1\lambda^2} + O(1), -\frac{G_1}{vC} + O\left(\frac{1}{v^2}\right) \qquad (v \sim \infty) \quad (31b)$$

In these limits (30) reduces respectively to

$$\frac{1}{2f}\left[-\left(1+\frac{vC}{2G_1\lambda}\right)e^{-(vt-x)}\theta(vt-x) + \left(1-\frac{vC}{2G_1\lambda}\right)e^{-(x-vt)}\theta(x-vt)\right] \qquad (32a)$$

and

$$\frac{1}{f}\left[-e^{-G_1(vt-x)/vC}\theta(vt-x) + \left(\frac{G_1^2\lambda^2}{v^2C^2}\right)e^{-vC(x-vt)/G_1\lambda^2}\theta(x-vt)\right] \qquad (32b)$$

These extreme cases are drawn in figure 7. It is interesting to note that the slight asymmetry for $v \sim 0$ in the heights of the upsurge and subsequent downsurge, in which the latter is slightly smaller than the former, is accentuated enormously as $v \sim \infty$. The downsurge is twice as large as when $v \sim 0$, whilst the upsurge decreases as $O\left(\frac{1}{v^2}\right)$. Moreover the rise and fall times are also highly asymmetrical, the former going to zero as $O\left(\frac{1}{v}\right)$, the latter increasing as O(v). All of these effects are to be expected on general grounds, the above asymmetry arising

[illegible] from the reduced time for the effects to be experienced

ahead of the step function as v increases, compared to the increased capacatative effects behind the step function.

(e) Harmonic inputs.

From eqn. (15)it is seen that

$$\tilde{V}_1 - \tilde{V} = 1 - \left[1 + \frac{i\omega C}{G_1} + \underline{k}^2\lambda^2\right]^{-1} \qquad (33)$$

This simple expression should be compared with experimental data on vertebrate retinae in the same manner, for example, as done for the limulus retina by Brodie et al (1978a,b).

The behaviour of $|\tilde{V}_1 - \tilde{V}|$ is shown for different $\underline{k}^2$ and w in fig 8.

DISCUSSION

It has been shown here that

(1) a mathematical framework can be constructed to describe the silicon analog model of early visual processing of Mead and Mahowald (1988)

(2) in the continuum limit of the lattice network used to model lateral inhibition, analytic solutions can be given both for the system transfer function and for the response to various simple forms of illumination (which agree with the analog model behaviour).

Such results indicate that a full-scale computer simulation of the basic equations (4) might lead to even better agreement with the analog results. Moreover there is now the possibility (as discussed in association with (6)) of modelling the response of lattices other than the simple nearest-neighbour hexagonal one. This may allow some elucidation of the connectivity between neurons in the vertebrate or invertebrate retina, by choosing the lattice structure which gives the closest fit to the known response of that retina.

It should be remarked here that, as discussed in the second section, the quantity λ for a net with general connectivity is given by

$$\lambda^2 = \frac{1}{4}\langle \underline{r}^2 \rangle \cdot \left(\frac{G_2}{G_1}\right) \qquad (34)$$

Therefore if it is possible to measure λ by the above effects in a living retina, and at the same time independently measure G_1 and G_2, then the mean-squared value of the distance over which horizontal cell connections are effective may be obtainable.

There is also the possibility of a hybrid model which combines the 'slow potential' approach considered here with a noisy neuron model presented earlier (Taylor 1972). The behaviour of such noisy networks has been discussed recently (Gorse and Taylor 1988a,1988b), and extended to a description of inhibitory effects in the lateral eye of limulus (Gorse and Taylor 1988c). This latter analysis did not take detailed account of the slow potential contributions. It should now be possible to combine the approach discussed in this paper with the earlier noisy neural model.

The author would like to thank Dr. D. Gorse for many helpful and stimulating discussions on visual processing.

References

Brodie, S.E., Knight, B.W. and Ratliff, F. (1978a). The spatiotemporal transfer function of the limulus lateral eye. J. Gen. Physiol. 72, 167-202.

Brodie, S.E., Knight, B.W. and Ratliff, F. (1978b). The response of the limulus retina to moving stimuli: a prediction by Fourier synthesis. J. Gen. Physiol. 72, 129-166.

Dowling, J. (1987). The retina: An approachable part of the brain. Cambridge MA; Harvard University Press.

Gorse, D. and Taylor, J.G. (1988a). On the equivalence and properties of noisy neural nets, Phys. Lett. A (in press).

Gorse, D. and Taylor, J.G. (1988b). An analysis of noise RAM and neural nets. King's College preprint Jan.1988.

Gorse, D. and Taylor, J.G. (1988c). A RAM net approach to visual processing in the limulus lateral eye.

Hartline, H.K. and Ratliff, F. (1972). Inhibitory interactions in the retina of limulus, in Handbook of Sensory Physiology, Vol.VII (Part 2, M.G. Guortes, editor, Springer-Verlag, Berlin 381-447.

Mead, C.A. and Mahowald, M.A. (1988). A silicon model of early visual processing. Neural Networks 1, 91-97.

Taylor, J.G. (1972). Spontaneous behaviour in neural networks. J. Theor. Biol. 36 513-528.

Figure Captions

Figure 1.

Schematic diagram of a cross-section through a vertebrate retina. R: photoreceptor, H: horizontal cell, B: bipolar cell, A: amacrine cell, G: ganglion cell.

Figure 2

Schematic diagram of a cross-section through an invertebrate retina (limulus polyphemus). R: photoreceptor, E: eccentric cell, R': retinular cell.

Figure 3

The silicon retina of Mead and Mahowald (1988). This is composed of a resistive network made of a hexagonal lattice. The single pixel element at each node is shown in the next figure.

Figure 4

(a) The circuit diagram of the single pixel element comprising each node of the hexagonal lattice of figure 3. V_1 is the generator potential arising from the photoreceptor, I_2 is the current carried by a capacitor, and I_3 the current flowing into the network at the node P.

(b) Current flow from one node to a neighbour in the resistive network.

Figure 5

(a) Response of a single pixel element to a step function illumination in time which covers the whole retina.

(b) Response as (a) but now to a step-function illumination in time only over a limited part of the retina.

Figure 6

The dependence of the response function (V_1-V), given by equation (28), to a circular patch of light of radius r_0, in the limits (a) $r_0 \sim 0$ and (b) $r_0 \sim \infty$.

Figure 7.

The response function (V_1-V) of equation (30) for the response to an illumination edge moving with velocity v in the limits (a) $v \sim 0$ (see equation) (32a) and (b) $v \sim \infty$ (see equation (32b).

Figure 8

The modulus of the response function $(\tilde{V}_1-\tilde{V})$, in Fourier transform space , given by equation (33), and plotted for varying $\underline{k}^2$, for different values of w.

FIGURE 1

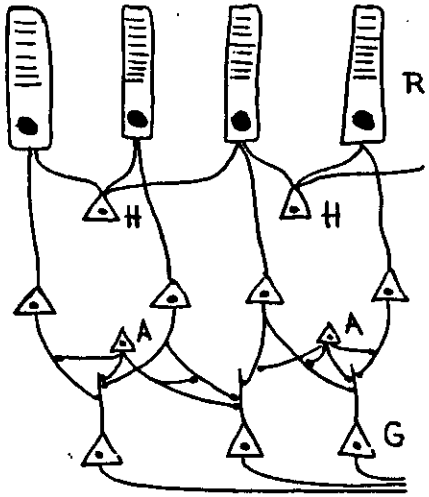

FIGURE 2

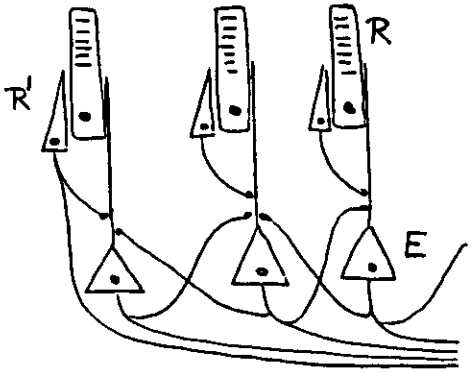

FIGURE 3

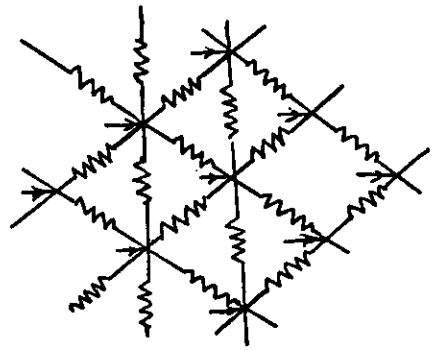

FIGURE 4

(a)

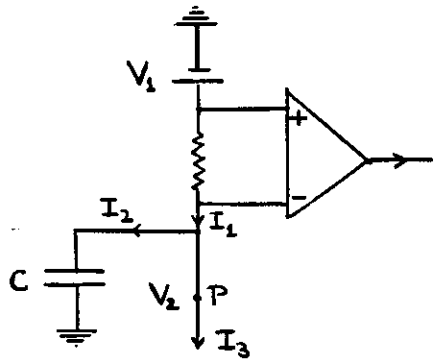

(b)

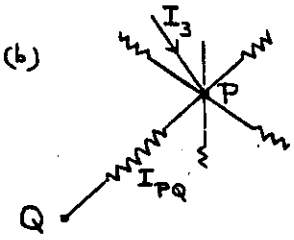

FIGURE 5

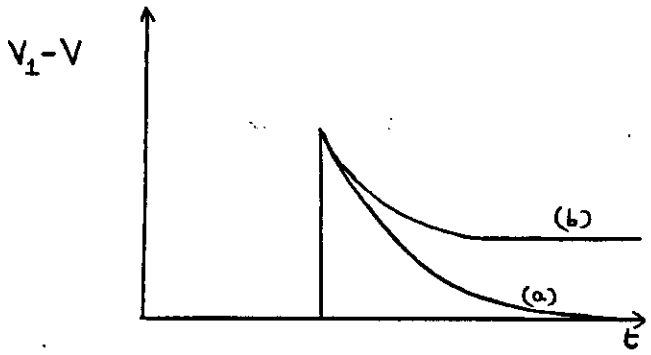

(a)

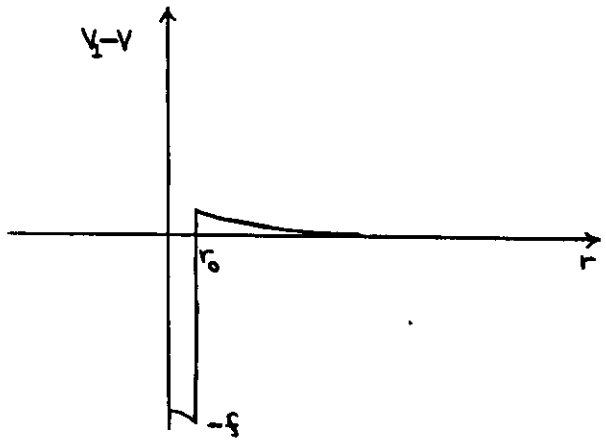

(b)

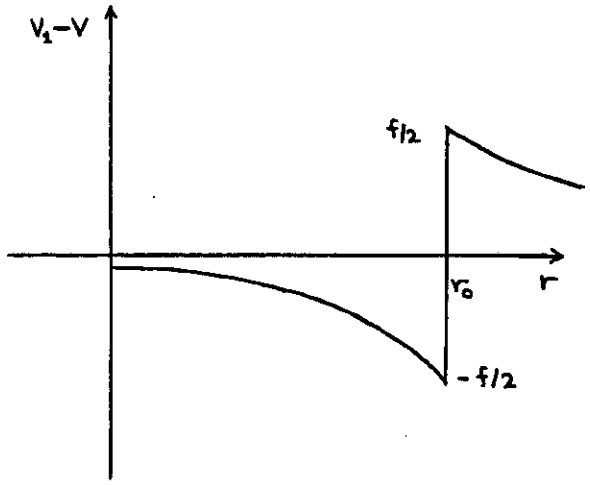

Figure 7

(a)

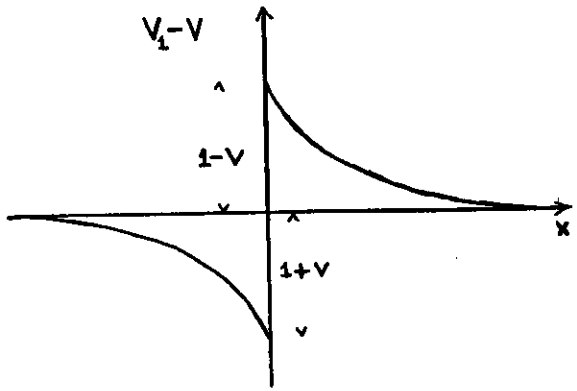

(b)

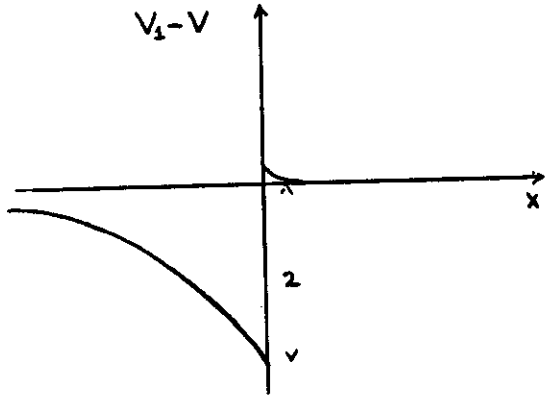

Figure 8